EFFECTS OF VEHICLE IMPACT VELOCITY AND FRONT-END STRUCTURE ON THE DYNAMIC RESPONSES OF CHILD PEDESTRIANS

Xuejun Liu and Jikuang Yang
Crash Safety Division, Chalmers University of Technology
412 96, Göteborg, Sweden

ABSTRACT

To investigate the effects of vehicle impact velocity and front-end structure on the dynamic responses of child pedestrians, an extensive parametric study was carried out by using four mathematical models including 3-, 6-, 9- and 15-year-old children. Within the parametric study, the impact velocity was varied from 30 to 40 km/h, while the geometric parameters and mechanical properties of vehicle front structure were varied to represent a variety of modern passenger cars. Effects and interactions of various factors were evaluated in terms of crucial injury parameters concerning head, chest, pelvis and lower extremity.

The results from factorial analysis indicate that head and lower extremity are at higher injury risks than other body regions. The actual injury distribution of a child pedestrian varies significantly with body size. Therefore, in order to appropriately characterize the dynamic responses of children, another elder child model between 9 to 15 years old has to be taken into account, together with the 6-year-old child.

Vehicle impact velocity is of the most significant effect on the injury risks of child pedestrians. A remarkable reduction of injury severity was observed as the impact velocity decreases from 40 to 30 km/h. Design parameters of vehicle front-end structures impose different effects on the dynamic responses of child pedestrians. Some conflicting effects have to be balanced in order to mitigate the injury risks of children across a wide age range.

KEYWORDS Child Pedestrian, Parametric Study, Impact Velocity, Vehicle Front-end Structure

CHILDREN UNDER 15 YEARS OLD account for a substantial proportion of pedestrian injuries and fatalities in vehicle-related accidents (NHTSA, 2000; Peng and Bongard, 1999), of which the age group of 5-9 year-old is exposed to the highest risk due to high accident involvement (Assailly, 1997; Fontaine and Gourlet, 1997; NHTSA, 2000).

The majority of children victims are struck from side by the front-end of passenger cars (Ashton, 1986; Ohashi, 1990). In general, lower extremity and head injuries occur most commonly in child pedestrian accidents (Peng and Bongard, 1999; Sturtz, 1976). The actual injury distribution of a child pedestrian varies with body size, vehicle impact velocity and vehicle front-end structure (Edwards and Green, 1999; Lucchini and Weissner, 1980; Mukul, 1983; Sturtz, 1980).

In previous studies, by means of physical experiments (Lucchini and Weissner, 1980; Sturtz, 1980) and mathematical simulation (Mukul, 1983), only the 6-year-old child was regarded as the representative of children under 15 years old. A quantitive analysis on the influences of body size is necessary to evaluate the effectiveness of the 6-year-old child to represent the general injury characteristics of other age groups. Furthermore, to design a pedestrian-friendly vehicle, the influences of vehicle front-end structure on the dynamic responses of children have to be clarified at different impact velocities.

In this study, in order to cover a wide age range, four mathematical models representing 3-, 6-, 9- and 15-year-old children (Liu and Yang, 2001) were adopted into an extensive parametric study. By altering impact velocity, vehicle front-end profile and mechanical properties, the effects and interactions of these factors were assessed in terms of crucial injury parameters concerning head, chest, pelvis and lower extremity.

METHODS AND MATERIAL

CHILD PEDESTRIAN MODELS - Fig. 1 shows the variation of body size of child pedestrian models at 3-, 6-, 9-, 15-year-old (hereafter referred as 3YOC, 6YOC, 9YOC and 15YOC, respectively where appropriate) comparing with the 50% adult male model. The basic anthropometrical data of these children models was generated by GEBOD program (TNO, 1999). The resistive stiffness of joints and contact properties of body segments were scaled down from those of validated adult pedestrian models (Yang, *et al.*, 2000). Differences in anatomical structures between adults and children, as well as the age-dependent properties of bone and ligament, were taken into account in the scaling processes. The validity of these mathematical models was evaluated by reconstruction of real world accidents (Liu and Yang, 2001).

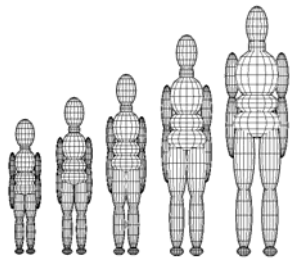

Fig. 1 Variation of body size of 3-, 6-, 9- and 15-year-old children and 50% adult male

VEHICLE MODEL - A baseline car model was formulated according to the front dimensions of VOLVO 850. It consists of four ellipsoids representing bumper, hood leading edge, hood top and windshield. Additional ellipsoids are attached to approximate the front-end profile. The definitions of important dimensions are illustrated in Fig. 2.

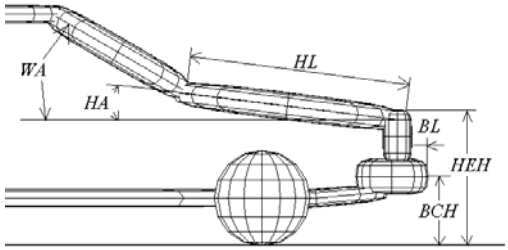

Fig. 2 Basic configuration and dimensions of the baseline car model, BCH=Bumper center height, BL=Bumper Lead Length, HEH=Hood Edge Height, HL=Hood Length, HA=Hood Angle, WA=Windshield Angle.

The force-deformation properties of bumper, hood leading edge and hood top were derived from the results of a sub-system test with VOLVO S70 (Fig. 3). The baseline (solid) stiffness property is chosen as the average of each corridor in loading phrase, while stiff (dash) and soft (dot) levels approximate the upper and lower margins, respectively.

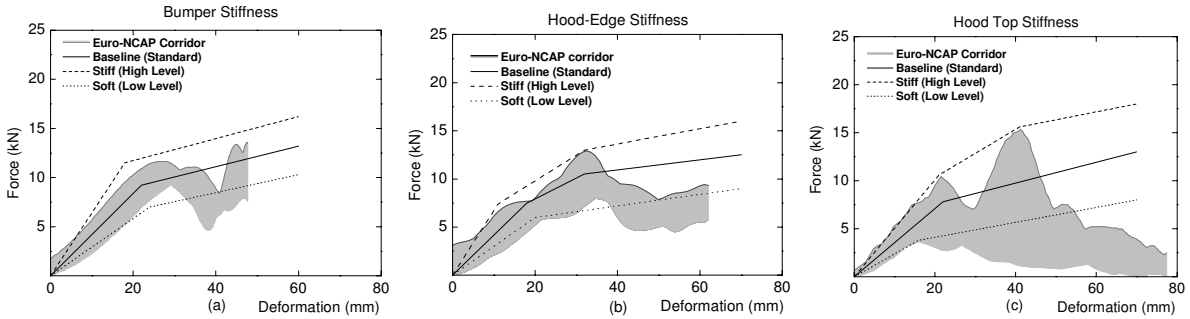

Fig. 3 Variation of stiffness properties (a) bumper, (b) hood leading edge, and (c) hood top surface.

DESIGN OF PARAMETRIC STUDY - The stiffness properties of vehicle front-end structure were varied according to the corridors (Fig. 3) obtained from sub-system tests, whereas the geometry was varied in accordance with front shape corridors of current production car models (Mizuno and Ishikawa, 2001). The selected parameters and corresponding variation levels were summarized in Table 1.

In a two-level factorial analysis (Box*, et al.*, 1978), the main effect of a factor is measured as the change in the average response as the factor varies from low to high levels. In a similar manner, the interaction effects among different factors can be estimated. Among all the possible interactions, two-factor interactions are of more interest than those higher-order ones in engineering analysis. In order to examine possible two-factor interactions without any confounding with main effects and higher order interactions, a half-fraction 2^{7-1} =64 was implemented with the generator I=ABCDEF for each child pedestrian model.

Table 1 Selected variables and variation levels

				Levels		
No.	Variable	Abbr.	Unit	Low	Baseline	High
A	Impact Velocity	VEL	km/h	30	-	40
B	Bumper Center Height	BCH	mm	320	400	480
C	Bumper Stiffness	BS	N/mm	300	420	640
D	Bumper Leading	BL	mm	80	100	120
E	Hood Edge Height	HEH	mm	560	740	840
F	Hood Edge Stiffness	HES	N/mm	300	416	600
G	Hood Top Stiffness	HTS	N/mm	250	350	500

INJURY PARAMETERS AND TOLERANCE LEVELS - Since very limited biomechanical data has been obtained directly from children biological experiments, various indirect methods had been employed to develop the injury tolerance levels of children (Kleinberger*, et al.*, 1998; Klinich*, et al.*, 1996; Sturtz, 1980). The injury parameters and corresponding tolerance levels used in this study were summarized in Table 2.

Table 2. Selected injury parameters and corresponding tolerance levels

Injury Parameter	Abbr.	Unit		Tolerance Level	References
HIC	HIC	-	-	900-1000	Kleinberger, et al.(1998)
Head Angular Acc.	HAA	3 ms	rad/s^2	8300-9100	Sturtz (1980)[direct loading]
Res. Chest Acc.	Chest	3 ms	g	55-73	Klinich, et al. (1996)
Res. Pelvis Acc.	Pelvis	3 ms	g	60	
Res. Femur Acc.	Femur	3 ms	g	150	
Res. Tibia Acc.	Tibia	3 ms	g	150	EEVC (1998)

RESULTS

OVERALL KINEMATICS AND DYNAMIC RESPONSES - To understand the injury distribution of child pedestrians and influences of body size, four simulations were performed with the baseline car model at impact velocity of 30 km/h. Only the primary impact against vehicle structure was considered, while the secondary impacts with ground was excluded. It aimed at providing a better understanding of the injury distribution of child pedestrians. This knowledge is also helpful to analyze the effects and interactions of other parameters.

3-year-old child - The initial impact occurs between bumper and upper leg (Fig. 4) resulting in 95.2 g in femur lateral acceleration at about 9 ms (Fig. 5a). At about 12 ms, pelvic resultant acceleration reaches its peak of 92.5 g due to the impact against bumper. Subsequently, chest is impacted by hood edge at about 23 ms leading to a peak of 73.8 g in chest acceleration (Fig. 5b). At the same time, head is subject to the impact against hood leading edge at head impact velocity of 29 km/h. The HIC value, head linear and angular accelerations are measured as 269, 62.5 g and 6021 rad/s^2, respectively. The primary impact ends up at about 50 ms.

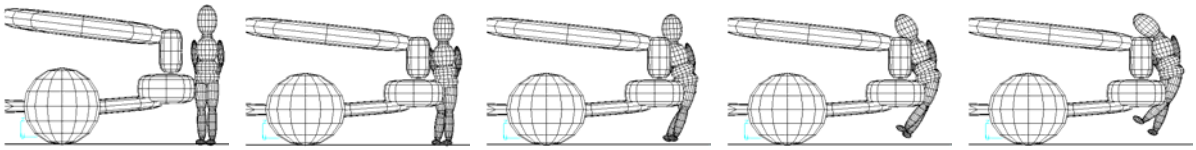

Fig. 4 Overall kinematics of the 3-year-old child impacted by the baseline car model at 30 km/h (0-40 ms, Δt=15 ms).

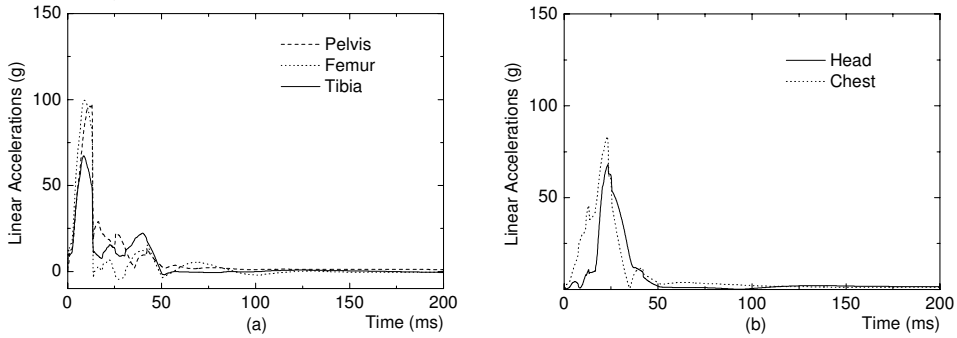

Fig. 5 Time histories of accelerations in (a) pelvis/femur/tibia and (b) head/chest of the 3-year-old child pedestrian model impacted by the baseline car model at 30 km/h

6-year-old child - The initial impact location is close to the lower part of right upper leg (Fig. 6). At about 8 ms from beginning, femur lateral acceleration has a peak loading of 79.6 g, while tibia acceleration is about 87.4 g (Fig. 7a). The pelvic resultant acceleration is about 40 g at 14 ms. Because of the impact against hood edge, chest area suffers an impact loading of 65.0 g at 29 ms (Fig. 7b). Then head begins to rotate downwards to the front part of hood top. The time history of head resultant acceleration indicates that the contact between head and hood top occurs at about 68 ms. The head impact speed is about 21.9 km/h. The simulated head injury parameters are HIC value of 259, 72.3 g in head linear acceleration and 5879 rad/s^2 in head angular acceleration. The whole process of primary impact ends up at about 100 ms.

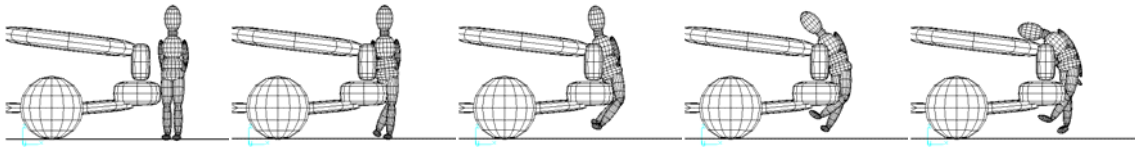

Fig. 6 Overall kinematics of the 6-year-old child impacted by the baseline car model at 30 km/h (0-60 ms, Δt=15ms)

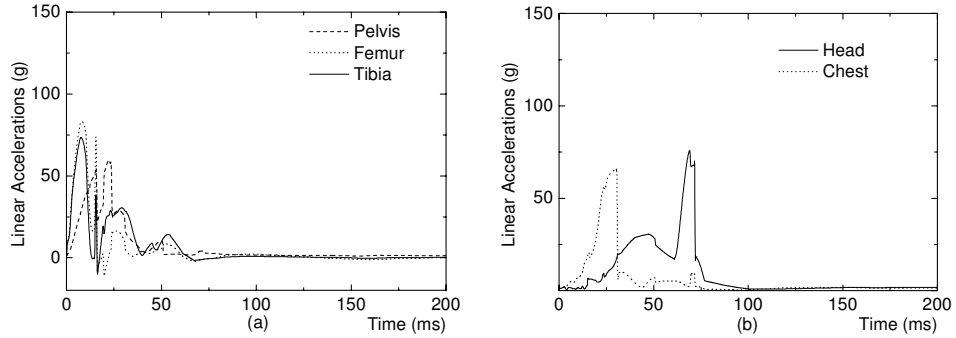

Fig. 7 Time histories of accelerations in (a) pelvis/femur/tibia and (b) head/chest of the 6-year-old child pedestrian model impacted by the baseline car model at 30 km/h.

9-year-old child - The initial impact location is just above the knee joint (Fig. 8). The peak values are about 80.5 g and 78.2 g at 9 ms for femur and tibia accelerations, respectively (Fig. 9a). At about 22 ms, the pelvic resultant acceleration reaches the peak of 86.1 g as a result of the contact with hood

leading edge. At about 24 ms, the peak value of chest resultant acceleration is about 23.0 g. Later, at around 86 ms, head resultant acceleration increases rapidly to the peak of 96.0 g (Fig. 9b) because of a direct impact against the front part of hood top at an impact speed of 31 km/h. HIC value is about 685, while the head angular acceleration is measured as 7671 rad/s^2. The primary impact ends up at about 105 ms.

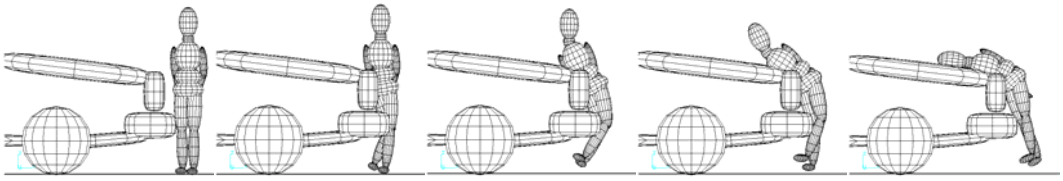

Fig. 8 Overall kinematics of the 9-year-old child impacted by the baseline car model at 30 km/h (0-80 ms, Δt=20ms)

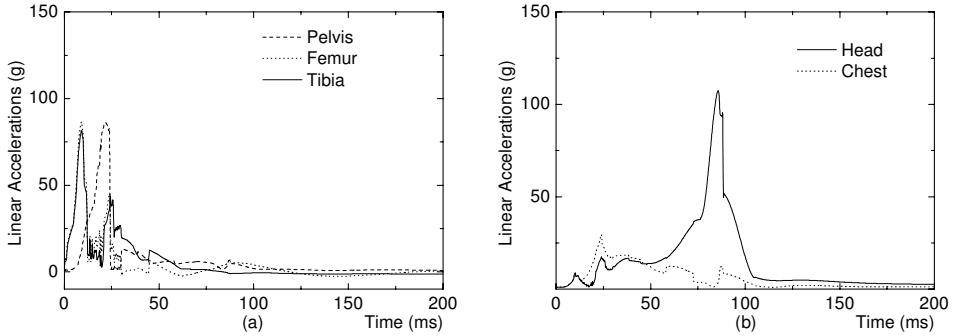

Fig. 9 Time histories of accelerations in (a) pelvis/femur/tibia and (b) head/chest of the 9-year-old child pedestrian model impacted by the baseline car model at 30 km/h.

15-year-old child - The initial impact location is just below the right knee joint (Fig. 10), resulting in peaks of 75.0 g and 51.8 g in tibia and femur accelerations, respectively (Fig. 11a). Pelvis area is subject to an impact loading of 48.5 g at about 29 ms. No direct impact between the chest and hood top is observed because of the interference by right upper arm. At about 126 ms, head hits the hood top surface at an impact speed of 31.4 km/h. The peaks of head linear and angular accelerations are 86.3 g (Fig. 11b) and 7364 rad/s^2, respectively, while HIC value is calculated as 654. The time duration of the primary impact is about 170 ms.

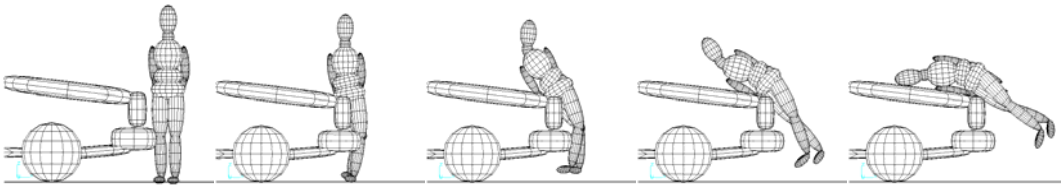

Fig. 10 Overall kinematics of the 15-year-old child impacted by the baseline car model at 30 km/h (0-120 ms, Δt=30ms)

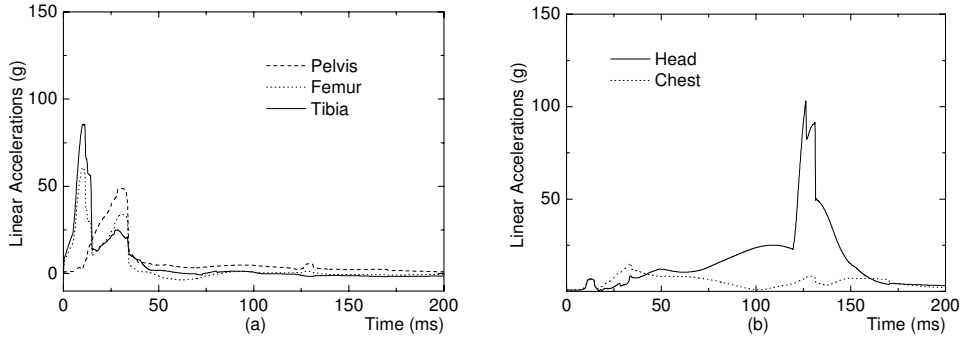

Fig. 11 Time histories of accelerations of (a) pelvis/femur/tibia and (b) head/chest of the 15-year-old child pedestrian model impacted by the baseline car model at 30 km/h.

EFFECTS OF VARIOUS PARAMETERS - The effects of vehicle impact velocity on the injury outcomes of child pedestrians were summarized in Table 3, in comparison with mean responses. The main effects and two-factor interactions of various parameters (Table 1) on the selected injury parameters (Table 2) were summarized in Table 4 to Table 7 for each child pedestrian separately.

Effect of vehicle impact velocity - As the vehicle impact velocity changes from 30 to 40 km/h, all injury parameters increase significantly, regardless of the age of child pedestrian. Head injuries, in terms of HIC value and head angular acceleration, can be significantly reduced at the impact velocity of 30 km/h. In other body areas, higher impact loadings are apparently associated with higher vehicle impact velocity.

Table 3. Main effects and mean responses of vehicle impact velocity from 30 to 40 km/h

	HIC		HAA (rad/s^2)		Chest (g)		Pelvis (g)		Femur (g)		Tibia (g)	
Age	Effect	Mean	Effect	Mean	Effect	Mean	Effect	Mean	Effect	Mean	Effect	Mean
3	1090.6	1500.4	1403	6960	29.1	69.1	34.4	96.8	33.2	104.7	37.3	102.8
6	565.5	568.6	3688	6478	22.8	50.1	30.5	77.3	30.9	89.2	40.3	121.3
9	537.9	605.5	2473	5625	11.3	35.9	26.9	66.8	25.1	75.2	33.3	117.6
15	1064.8	1423.3	2525	7071	7.6	24.2	17.3	46.6	21.8	63.0	29.8	102.2

Effects of vehicle front-end structure - For the 3-year-old child (Table 4), bumper center height (BCH) is significant to the responses of femur and tibia. By raising bumper center height from 320 to 480 mm, the lateral accelerations of tibia and femur decrease by 75.3 and 10.5 g, respectively. However, pelvic acceleration increases by 33.1 g at the same time. A compliant bumper structure can mitigate femur injury, and is insignificant to other regions. A more protruding bumper is preferable to reduce head injuries (-218.4 in HIC and -1811.2 rad/s^2 in HAA). Hood edge height has significant effects on the HIC value (+1576.4), chest acceleration (+34.7 g) and head impact velocity (+8.93 km/h). A compliant hood leading edge would be advisable to reduce head injury risks. No significant effect is associated with hood top stiffness. A careful combination of bumper center height and hood edge height could reduce the chest acceleration by 20 g, as well as the head impact speed by 3.79 km/h. The interaction (BL*HEH) between bumper lead length (BL) and hood edge height (HEH) could reduce the head angular acceleration by 1022.5 rad/s^2. Moreover, the interaction (HEH*HES) between hood edge height (HEH) and hood edge stiffness (HES) can also aggravate the head injuries (+451.7 in HIC and +1068.1 rad/s^2 in HAA).

Table 4. Effects and two-factor interactions on injury parameters of 3YOC

Effects and Interactions	Abbr.	HIC	HAA (rad/s^2)	Chest (g)	Pelvis (g)	Femur (g)	Tibia (g)	HSP (km/h)
BCH	B	440.7	4535.0	1.9	33.1	-10.5	-75.3	4.43
BS	C	-45.4	-8.8	-2.7	8.5	12.7	9.0	-0.73
BL	D	-218.4	-1811.2	12.9	5.7	1.5	-0.5	-1.75
HEH	E	1576.4	-279.4	34.7	-3.3	-0.5	-0.3	8.93
HES	F	528.6	989.4	4.9	0.3	0.0	-0.1	-0.16
HTS	G	69.0	471.9	-0.1	0.2	0.0	0.0	-0.00
BCH*BL	BD	-111.9	-1283.1	-1.7	-5.3	-1.4	-0.4	-1.01
BCH*HEH	BE	-259.2	-255.0	-20.0	4.1	0.9	-0.7	-3.79
BL*HEH	DE	-20.6	-1022.5	6.0	-3.3	-0.7	-0.2	0.13
HEH*HES	EF	451.7	1068.1	3.9	-0.6	0.0	-0.1	0.18
	Mean	1500.4	6960	69.1	96.8	104.7	102.8	32.0
	10% of Mean	150	696	6.9	9.7	10.5	10.3	3.2
	Standard Error	48.9	208.2	1.3	1.0	0.3	0.3	0.22

For the 6-year-old child (Table 5), bumper center height (BCH) controls the impact loading to lower extremity and the head angular acceleration. A higher bumper could reduce the tibia acceleration by 46.2g but increase the femur and pelvic accelerations by 20 and 31.5 g, respectively. At same time, the head angular acceleration increases by 1632.8 rad/s^2. A more compliant bumper structure can reduce the injury severity of lower extremity without any significant effects on other body regions. The only significant effect of bumper lead length is on the pelvic acceleration. A short

bumper is helpful to reduce pelvis loading by 11.5 g. The hood edge height (HEH) is responsible for the injury severities of head, chest and pelvis areas. For instance, a higher hood leading edge could reduce the HIC by 566, head angular acceleration by 1272.2 rad/s^2 and pelvic acceleration by 17.5g, but increase chest acceleration by 28.6 g. The stiffness property of hood leading edge (HES) is only relevant to chest acceleration. Except for the HIC value (+165.5) and head angular acceleration (+1163.5 rad/s^2), no other significant effect is associated with hood top stiffness. Additionally, significant interactions (BCH*BS) are detected between bumper center height (BCH) and bumper stiffness (BS) on the impact loadings to pelvis and femur. Meanwhile, bumper center height (BCH) also interacts with hood edge height (HEH) on the pelvic loading (+20.5 g).

Table 5 Effects and two-factor interactions on injury parameters of 6YOC

Effects and Interactions	Abbr.	HIC	HAA (rad/s^2)	Chest (g)	Pelvis (g)	Femur (g)	Tibia (g)	HSP (km/h)
BCH	B	177.4	1632.8	-5.2	31.5	20.0	-46.2	5.84
BS	C	-82.5	-122.8	-2.8	11.4	23.2	18.4	-1.02
BL	D	22.4	515.3	6.9	11.5	2.1	0.7	-0.92
HEH	E	-566	-1272.2	28.6	-17.5	1.1	0.8	-2.35
HES	F	-45.5	-280.3	10.2	7.7	-0.5	-0.9	-0.99
HTS	G	165.5	1163.5	0.0	-0.3	-0.7	-0.8	-0.04
BCH*BS	BC	-61.5	102.8	0.3	19.8	11.0	11.2	-0.44
BCH*HEH	BE	49.1	-360.3	-6.4	20.5	1.3	0.7	3.35
	Mean	568.6	6478.0	50.1	77.3	89.2	121.3	33.48
	10% of Mean	56.9	647.8	5.0	7.7	8.9	12.1	3.3
	Standard Error	32.2	293.6	1.0	2.1	0.7	0.9	0.36

For the 9-year-old child (Table 6), a higher bumper can be helpful to reduce the impact loading of tibia by 55 g. Bumper stiffness (BS) is significant on the impact loading of lower extremity. No significant influence is associated with bumper lead length. Although a higher hood edge (HEH) is aggressive to the chest, pelvis and femur areas, but it is helpful to mitigate head injuries in terms of the HIC value (-596.1) and head angular acceleration (-1936.3), and can result in a remarkable reduction of the head impact speed (-14.11 km/h). Except for slight effects on the chest and pelvis responses, hood edge stiffness (HES) is insignificant to other injury parameters. The stiffness of hood top surface (HTS) has slight effect on the HIC value (+198.9) but significant influence on the head angular acceleration (+1577.5). The interaction (HEH*HTS) between hood edge height (HEH) and hood top stiffness (HTS) is significant on the HIC value (-115.6).

Table 6 Effects and two-factor interactions on injury parameters of 9YOC

Effects and Interactions	Abbr.	HIC	HAA (rad/s^2)	Chest (g)	Pelvis (g)	Femur (g)	Tibia (g)	HSP (km/h)
BCH	B	57.7	652.5	0.4	-6.1	-4.7	-55.0	1.77
BS	C	-70.1	-552.5	-0.8	0.1	11.8	19.6	-1.03
BL	D	19.6	116.2	0.9	5.9	3.3	-1.0	0.43
HEH	E	-596.1	-1936.3	31.1	31.3	7.8	-2.2	-14.11
HES	F	-34.1	-68.1	6.9	10.2	1.3	-0.3	-0.81
HTS	G	198.9	1577.5	0.1	0.5	-0.4	0.0	-0.13
BCH*HEH	BE	75.3	413.7	-1.5	-11.2	3.3	-2.1	2.27
HEH*HTS	EG	-115.6	-361.2	-0.1	-0.2	-0.3	-0.1	-0.13
	Mean	605.5	5625.0	35.9	66.8	75.2	117.6	28.82
	10% of Mean	60.6	562.5	3.6	6.7	7.5	11.8	2.9
	Standard Error	11.0	72.9	0.5	1.1	0.4	0.2	0.14

In the case of 15-year-old child (Table 7), a higher bumper could significantly reduce the tibia loading (-33.3 g). This can be explained as the impact location of bumper moves above the knee joint. A soft bumper structure (BS) is helpful to reduce the tibia acceleration by 18 g without any significant effect on other injury parameters. Hood edge height (HEH) has significant effect on the head angular acceleration. By raising hood edge height from 560 to 840 mm, the head angular acceleration (HAA) increases by 2484.7 rad/s^2, whereas the head impact speed (HSP) decreases by 4.52 km/h. Additionally, the pelvic acceleration increases by 54.6 g with a higher hood edge. Hood edge stiffness

(HES) has no outstanding effect on all injury parameters. Hood top stiffness (HTS) is responsible for severe head injuries (+482.1 in HIC and 2145.9 rad/s^2 in HAA). Apparent interactions between bumper center height and hood edge height are detected in terms of the HIC value (+407.5), head angular acceleration (+1109.7 rad/s^2), as well as the head impact speed (+4.68 km/h).

Table 7 Effects and two-factor interactions on injury parameters of 15YOC

Effects and Interactions	Abbr.	HIC	HAA (rad/s^2)	Chest (g)	Pelvis (g)	Femur (g)	Tibia (g)	HSP (km/h)
BCH	B	-136.5	-294.7	0.0	3.0	14.0	-33.3	-2.27
BS	C	-134.8	-238.4	-0.5	-1.5	7.8	18.0	-0.75
BL	D	-75.3	-253.4	0.5	0.4	6.9	1.0	-0.45
HEH	E	-21.3	2484.7	3.2	54.6	7.4	-0.6	-4.52
HES	F	-143.3	-413.4	0.9	5.9	2.2	-0.8	-1.05
HTS	G	482.1	2145.9	3.0	0.8	0.3	1.5	-0.30
BCH*HEH	BE	407.5	1109.7	2.0	0.8	-3.0	2.4	4.68
	Mean	1432.3	7071.4	24.2	46.6	63.0	102.2	41.11
	10% of Mean	143.2	707.1	2.4	4.7	6.3	10.2	4.1
	Standard Error	45.8	110.1	0.4	0.9	0.7	1.6	0.11

DISCUSSIONS

VALIDITY OF CHILD PEDESTRIAN AND VEHICLE MODELS: The biofidelity of child pedestrian models is an essential aspect of this parametric study. However, in the absence of sufficient biomechanical data of children, the validity of these child pedestrian models was only evaluated by means of accident reconstruction (Liu and Yang, 2001). Further studies are necessary to validate and improve the biofidelity of these child pedestrian models. Additionally, the validity of vehicle model is also an important aspect. In this study, the variation range of stiffness properties of vehicle front-end structure is solely based on one set of sub-system test results with a specific car model. It is also desirable to include other production car models. Furthermore, the variation of front-end shape is intended to represent current passenger cars. Other vehicle types, such as vans and trucks, are excluded.

ESTIMATION OF SIGNIFICANCE OF EFFECTS AND INTERACTIONS: To determine the significance of an effect, the standard error of the effect should be estimated in advance. Since there is no random variability in current mathematical simulations, the standard errors were estimated from higher-order interactions. However, such standard errors are usually too small to be of engineering interest. By analyzing the results from full-scale pedestrian crash tests, Mukul (1983) proposed an average coefficient of variation (the ratio of standard deviation to the mean) as 24% to evaluate the significances of various injury parameters, which are primarily related to linear accelerations. No suggestion was given to other measurements, such as head angular acceleration and head impact speed. Hence, in this study, the average coefficient of variation was chosen as 10% of the mean response in order to have a uniform criterion for different types of measurement.

INJURY CRITERIA: To evaluate injury risks of child pedestrian, it is essential to have certain tolerance levels. Unfortunately, the injury criteria and tolerance levels of children have not yet been well established. Various studies have suggested considerably different tolerance levels by means of different approaches (Klinich, et al., 1996). Nevertheless, the purpose of this study was not to measure the actual injury severity, but to evaluate the effects of different parameters. Thus, the tolerance levels in Table 2 were only considered as references.

To measure the head and brain injury risks, HIC value takes into account the translational aspect of head motion, whereas the head angular acceleration is to assess the rotational aspect. In this study, the 3 ms clip of 8300-9100 rad/s^2 (Sturtz, 1980) was regarded as the criterion of head angular acceleration. This is mainly due to the fact that, in most of current mathematical simulations, the child's head suffers from a direct impact loading by the vehicle front structure. In further study, the

DAI thresholds (Margulies and Thibault, 1991), expressed in a relationship between the head angular acceleration and change in angular velocity, will be used to evaluate brain injuries.

For lower extremity, it is more appropriate to use bending moment and impact force to predict injury risks. However, due to the limitation of current mathematical models, the bending motion of lower extremity cannot be properly simulated. Hence, only the 3 ms clips of lateral accelerations were considered.

INFLUENCE OF BODY SIZE: The influence of body size can be clearly explained by the comparison of overall kinematics and dynamic responses (Fig. 4 to Fig. 11). The initial impact location is determined by the relative height of child victim to vehicle front-end structure. For younger children under 6 years old, the initial impact occurs between bumper and upper leg area, whereas for elder children above 6 years old, the initial impact is close to knee joint. Furthermore, due to the shorter stature, younger children are exposed to higher impact loading by bumper and hood leading edge in pelvis and chest areas. Another obvious difference in overall kinematics is that, younger children are almost pushed straightly forward with little rotational movement, whereas elder children tend to wrap around hood leading edge.

The differences mentioned above indicate that the 6-year-old child alone cannot adequately represent elder children between 9 and 15 years old. Therefore, it is necessary to consider one elder child model between 9-15 year-old together with the 6-year-old model to design a real pedestrian-friendly vehicle.

EFFECTS OF VEHICLE IMPACT VELOCITY: It is not surprising that vehicle impact velocity plays a dominant role in the injury severity of child pedestrians. One can draw such a conclusion intuitively. However, a quantitive analysis can be helpful for traffic administrations to adjust their traffic regulations when child pedestrians are concerned. Based on real world accident data, Appel*, et al.* (1975) concluded that the mean impact speed in fatal and non-fatal pedestrian accidents is 34 km/h. However, this result is affected by old car models of 1970s'. A more recent study (Takeuchi*, et al.*, 1998) compared the changes in the incidence and consequences of car-pedestrian accidents in urban traffic during a ten-year period. The authors stated that the average injury severity of child pedestrians reduced by 50%, while that of elderly pedestrians by 39%. One of the major reasons was pointed out as the reduction of vehicle travel speed within the city center. In this study, the effects of vehicle impact velocity (Table 3) reasonably agree with the findings in previous studies especially in terms of head injuries. A significant reduction of overall injuries was observed as the vehicle impact velocity decreases from 40 to 30 km/h.

EFFECTS OF VEHICLE FRONT-END STRUCTURE: For child pedestrians at different ages, the design parameters of vehicle front structure can impose different and even controversial effects on various injury parameters. For instance, hood edge height is an important parameter for all injury parameters. A higher hood edge can reduce HIC value, head angular acceleration significantly of the 6- and 9-year-old children. On the contrary, it can aggravate the HIC value of the 3-year-old and the head angular acceleration of the 15-year-old child. In the case of adult pedestrian (Liu*, et al.*, 2002), a higher hood edge can significantly reduce the head impact velocity. However, no result was given about the dependency of head angular acceleration on the hood edge height for the adult pedestrian. Another interesting parameter is the bumper center height. For the 3- and 6-year old children, a higher bumper results in higher impact loadings to head and pelvis areas, but decreases the tibia lateral acceleration significantly. For elder children such as 9- and 15-year old, the bumper center height only relates to the lower extremity injuries.

Some significant interactions were also detected. For instance, the height and stiffness of hood edge interact with each other on the HIC value and head angular acceleration of 3-year-old child. For 15-year-old child, the interactions between bumper center height and hood edge height are significant on HIC and head angular acceleration. All these two-factor interactions make the injury prevention of child pedestrian even more complicated.

GENERAL REMARKS: To design a pedestrian-friendly vehicle is a challenge to automobile industry. Difficulties arise from the variation of accident circumstances, but more importantly from the differences in pedestrian victims. As shown in Fig. 4 to Fig. 11, even though with the same baseline car model at same impact velocity of 30 km/h, the injury distribution varies significantly for children aged between 3 and 15 years old. Therefore, considering the children between 3 and 15 years old, it seems very difficult to reach an optimal design for all interested injury parameters. In a strict sense, such an optimal solution does not exist. A practical idea for such a complex problem is to find a balance among all these injury parameters of child pedestrians at different ages. Such a balance can probably be approached by using the stochastic analysis, which recently has been successfully applied to find robust solutions in crash and injury prevention problems (Marczyk, 1999).

CONCLUSIONS

Injury distribution of child pedestrian varies significantly with body size. Head and lower extremity are under higher impact loading than other regions. For children under 6 years old, chest and pelvis areas are exposed to higher injury risks than elder children above 6 years old, whereas elder children receive more severe injury to head. To design a pedestrian-friendly vehicle, another elder child model between 9 and 15 years old should be involved along with the conventional 6-year-old model.

Vehicle impact velocity is the most significant factor on the injury severity of children. A remarkable reduction of injury severity was observed as the vehicle impact velocity varies from 40 to 30 km/h. The results from factorial analysis indicate that various parameters have different effects on the dynamic responses of child pedestrians. Some conflicting effects have to be balanced in order to mitigate the injury severity of child pedestrians across a wide age range.

Further parametric study will be carried out by using the stochastic analysis method. Three adult models (i.e. 5^{th} percentile female, 50^{th} and 95^{th} percentile male) and three child models (i.e. 3-, 6- and 9-year old) will be involved within a random simulation scheme.

ACKNOWLEDGEMENTS

This study was sponsored by the Swedish National Road Administration (Vägverket) and partly by the Autoliv Research and Development.

REFERENCES

Appel, H., Stürtz, G. and Gotzen, L. (1975) Influence of Impact Speed and Vehicle Parameter on Injuries of Children and Adults in Pedestrian Accidents, *Proc. Int. IRCOBI Conf. Biomechanics Impacts*, pp.83-100.

Ashton, S. J. (1986) Child Occupant and Child Pedestrian Leg Injuries, *Symposium on Biomechanics and Medical Aspects of Lower Limb Injuries, P-186*, SAE Paper 861929, pp.115-128.

Assailly, J. P. (1997) Characterization and Prevention of Child Pedestrian Accidents: An Overview, *Journal of Applied Developmental Psychology*, Vol. **18**(2), pp.257-262.

Box, G. E. P., G.Hunter, W. and Hunter, J. S. (1978) Statistics for Experimenters - An Introduction to Design, Data Analysis, and Model Building, John Wiley & Sons, New York.

Edwards, K. J. and Green, J. F. (1999) Analysis of the Inter-relationship of Pedestrian Leg and Pelvis Injuries, *Proc. Int. IRCOBI Conf. Biomechanics Impacts*, pp.355-369.

EEVC (1998) Improved Test Methods to Evaluate Pedestrian Protection Afforded by Passenger Cars, Report, European Enhanced Vehicle-Safety Committee, Working Group 17.

Fontaine, H. and Gourlet, Y. (1997) Fatal Pedestrian Accidents in France: A Typological Analysis, *Accident Analysis & Prevention*, Vol. **29**(3), pp.303-312.

Kleinberger, M., Sun, E. and Eppinger, R. (1998) Development of Improved Injury Criteria for the Assessment of Advanced Automotive Restraint Systems, Report, U.S. Department of Transportation, National Highway Traffic Safety Administration.

Klinich, K. D., Saul, R. A., Auguste, G., Backaitis, S. and Kleinberger, M. (1996) Techniques for Developing Child Dummy Protection Reference Values, Report, U.S. Department of Transportation, National Highway Traffic Safety Administration.

Liu, X. J. and Yang, J. K. (2001) Development of Child Pedestrian Mathematical Models and Evaluation with Accident Reconstructions, *Proc. Int. IRCOBI Conf. Biomechanics Impacts*, pp.103-113.

Liu, X. J., Yang, J. K. and Lövsund, P. (2002) A Study of Influences of Vehicle Speed and Front Structure on Pedestrian Impact Responses using Mathematical Models, *Traffic Injury Prevention*, Vol. **3**(1), pp.31-42.

Lucchini, E. and Weissner, R. (1980) Differences between the Kinematics and Loading of Impacted Adults and Children: Results from Dummy Tests, *Proc. Int. IRCOBI Conf. Biomechanics Impacts*, pp.165-179.

Marczyk, J. (1999) Principles of Simulation-Based Computer-Aided Engineering, FIM Publications, Barcelona, Spain.

Margulies, S. S. and Thibault, L. E. (1991) A Proposed Tolerance Criterion for Diffuse Axonal Injury in Man, *Journal of Biomechanics*, Vol. **25**(8), pp.917-923.

Mizuno, Y. and Ishikawa, H. (2001) Summary of IHRA Pedestrian Safety WG Activities - Proposed Test Methods to Evaluate Pedestrian Protection Afforded by Passenger Cars, *Proc. 17th Int. Technical Conf. on Enhanced Safety Vehicle,* pp.1-17.

Mukul, K. V., Repa, B S. (1983) Pedestrian Impact Simulation - A Preliminary Study, *Proc. 27th Stapp Car Crash Conf.*, SAE Paper 831601, pp.15-30.

NHTSA (2000) Traffic Safety Facts - Children, Report, National Highway Traffic Safety Administration, Department of Transportation, U.S.A.

Ohashi, H., Ono, K., Sasaki, A., Ohashi, N., Misawa, S. (1990) The Present Situation of Pedestrian Accidents in Japan, *Proc. Int. IRCOBI Conf. Biomechanics Impacts*, pp.283-292.

Peng, P. Y. and Bongard, F. S. (1999) Pedestrian Versus Motor Vehicle Accidents: An Analysis of 5,000 Patients, *Journal of the American College of Surgeons*, Vol. **189**(4), pp.343-348.

Sturtz, G. (1980) Biomechanical Data of Children, *Proc. 24th Stapp Car Crash Conf.*, SAE Paper 801313, pp.511-559.

Sturtz, G., Suren, E G., Gotzen, L., Behrens, S., Richter, K. (1976) Biomechanics of Real Child Pedestrian Accidents, *Proc. 20th Stapp Car Crash Conf.*, SAE Paper 760814, pp.465-510.

Takeuchi, K., Bunketorp, O., Ishikawa, H. and Kajzer, J. (1998) Car-pedestrian Accidents in Gothenburg during Ten Years, *Proc. Int. IRCOBI Conf. Biomechanics Impacts*, pp.87-98.

TNO (1999) *MADYMO User's Manual 3D. Version 5.4,* TNO Road-Vehicles Research Institute, Delft, The Netherlands.

Yang, J. K., Lövsund, P., Cavallero, C. and Bonnoit, J. (2000) A Human-Body 3D Mathematical Model for Simulation of Car-Pedestrian Impacts, *Journal of Crash Prevention and Injury Control*, Vol. **2**(2), pp.131-149.